Structural analysis and atomic simulation of Ag/BN nanoparticle hybrids obtained by Ag ion implantation

CrossMark

K.L. Firestein [a], D.G. Kvashnin [a], A.N. Sheveyko [a], I.V. Sukhorukova [a], A.M. Kovalskii [a], A.T. Matveev [a], O.I. Lebedev [b], P.B. Sorokin [a,c,*], D. Golberg [d,**], D.V. Shtansky [a,**]

[a] National University of Science and Technology "MISIS", Leninsky prospect 4, Moscow 119049, Russian Federation
[b] CRISMAT, UMR 6508, CNRS-ENSICAEN, 6Bd Marechal Juin, Caen 14050, France
[c] Technological Institute of Superhard and Novel Carbon Materials, 7a Centralnaya Street, Troitsk, Moscow 142190, Russian Federation
[d] National Institute for Materials Science (NIMS), Namiki 1, Tsukuba, Ibaraki 3050044, Japan

ARTICLE INFO

ABSTRACT

The present paper describes fabrication of Ag/BN nanoparticle hybrids by means of Ag ion implantation into the hollow BN nanoparticles (BNNPs) with a petal-like surface. The structural transformations occurring during Ag ion implantation into BNNPs are studied by low- and high-resolution transmission electron microscopy (TEM), high angle annular dark field scanning TEM (HAADF-STEM) paired with energy-dispersive X-ray (EDX) spectroscopy mapping. The experimental results are theoretically verified in the framework of the classical molecular dynamics (MD) method. Our results have demonstrated that by changing Ag ion energy in the range of 2–20 kV it is possible to selectively fabricate Ag/BNNP nanohybrids with crystalline or amorphous BNNP structures and various Ag NPs distributions over the BNNP thicknesses.

© 2016 Elsevier Ltd. All rights reserved.

1. Introduction

Synthesis and application of boron nitride (BN) nanomaterials is an exciting and rapidly developing area. BN nanostructures have attracted significant attention due to their rich functionality in reinforcement ultralight metals [1–3] and ceramics [4], improvement thermal conductivity and mechanical strength of polymers [5], making transparent superhydrophobic films [6], creating drug delivery systems [7], and many other applications [8]. There has been also a comprehensive scientific interest in the development and fabrication of BN-based composites for many structural, functional, and medical applications [9,10]. While consisting of dissimilar materials with completely different characteristics such composites can possess a unique combination of properties superior to those of individual components.

Due to the unique sp^2-bonded structure, chemical inertness, inherent hydrophobic nature, and biocompatibility the BN nanomaterials can particularly be used as smart platforms for drug delivery systems. The surface functionalization is an important intermediate step toward their efficient chemotherapeutic performance. In order to minimize the toxic effect on healthy cells to increase efficacy and improve selectivity of cancer therapy, the BN nanocarriers should be conjugated to a tumor-cell-specific small-molecule ligands for affecting tumor receptors [11,12]. After loading the antitumor drug, the BN nanomaterials can be accumulated into tumors in vivo through "active" targeting by recognition of specific receptors actively expressed on the cancer cell surfaces.

The direct cross-linking of targeting ligands or other biological molecules to BN nanomaterials is impeded due to the inherent BN hydrophobicity. In order to overcome this problem, metallic linkers, such as gold or silver nanoparticles (NPs), can be used [13]. These noble metals can be easily functionalized through Ag-S (or Au-S) interactions which facilitate the binding of biological molecules using various thiol linkers [14]. Other exciting applications of BN/noble metal composites include the fabrication of quantum electronic devices [15] and catalyst supports. For instance, Ag NPs-loaded BN sponges [16] and BN nanosheets supporting noble metal NPs were proposed as catalysts for methanol combustion [17] and for the reduction of *p*-nitrophenol [18].

Ag/BN nanohybrids are also of great interest as photocatalysts, molecular probe sensors [19,20], pollutant capturing surface enhanced Raman spectroscopy substrates [21], and antibacterial agents [22]. The use of Ag as bactericidal element is a prospective and rapidly emerging field. We note, however, that Ag NPs are easily aggregated in a solution. This leads to deterioration of their chemical properties and loss of antibacterial activity [23,24]. Thus the use of various Ag NPs supporting

---

* Correspondence to: P.B. Sorokin, National University of Science and Technology "MISIS", Leninsky prospect 4, Moscow 119049, Russian Federation.
** Corresponding authors.
E-mail addresses: pbsorokin@misis.ru (P.B. Sorokin), golberg.dmitri@nims.go.jp (D. Golberg), shtansky@shs.misis.ru (D.V. Shtansky).

substrates and BN nanosheets, in particular [25], can not only help to overcome this problem, but also contribute to achieving better antimicrobial activity compared with individual NPs [26–28].

To date BN/Ag nanohybrids have mainly been produced by decomposition of AgNO₃ in suspension of BN nanostructures under microwave or ultraviolet radiations [19,29]. The method of Ag/BN nanosheets fabrication by reduction of silver acetate hydrazine in the presence of BN was also utilized [25]. Ion implantation has widely been used to modify the surface of various materials under a close control of the doped element dosage [30]. It is worth noting that for BN nanomaterials the number of such studies has been limited. Multi-walled BN nanotubes (BNNTs) were irradiated with low and medium energy argon and helium ions at room and elevated temperatures [31]. It was also shown that by changing the ion-implantation parameters it is possible to fabricate BNNTs/metal composites with different contents of BN crystalline phase controlled morphologies, structures and volume fraction of metal phase additives [32].

The hollow BN NPs (BNNPs) with a petal-like surface have a number of advantages over their bulky counterparts due to the high specific surface area, high blind porosity, and low density. The present paper is focused on the fabrication of Ag/BNNP nanohybrids. And then the structural transformations occurring during Ag ion implantation into BNNPs were studied both theoretically and experimentally.

2. Experimental and theoretical methods

2.1. Experimental details

The BNNPs with an average external diameter of 100 nm were prepared by chemical vapor deposition (CVD) using boron oxide vapor and flowing ammonia reaction in a vertical induction furnace, as described elsewhere [7]. The powder mixture of FeO, MgO, and B (all of an analytical grade) prepared at a weight ratio of 150:28:75 was used as a boron oxide source. The BN ceramic crucible was filled with the powder mixture and put into the heating zone of a BN reactor. Boron oxide vapor, as a source of B for the CVD reaction with ammonia gas (99.98%), was generated during the following oxidation reactions within the precursor:

$$2B\ (s) + 2MgO\ (s) \rightarrow B_2O_2\ (g) + 2\ Mg\ (g) \tag{1}$$

$$2B\ (s) + 2SnO\ (s) \rightarrow B_2O_2\ (g) + 2Fe\ (g). \tag{2}$$
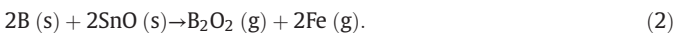
Boron oxide vapor was transported to the reaction zone with ammonia by an argon flow. BNNPs were synthesized using the following reaction of boron oxide vapor with ammonia:

$$B_2O_2\ (g) + 2NH_3\ (g) \rightarrow 2BN\ (s) + 2H_2O\ (g) + H_2\ (g). \tag{3}$$
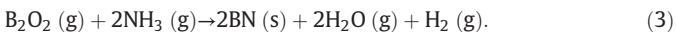
In order to separate the agglomerates into individual nanoparticles, after the synthesis the BNNPs were hand-grinded in an agate mortar. Then a drop of BNNPs suspension was dripped onto a TEM Cu grid, 3 mm in diameter, having 15–25 nm thick supporting holey carbon film (SCF). The individual BNNP structures were studied by a transmission electron microscopy (TEM) and electron diffraction (ED) using JEM-2100F (JEOL Ltd., Japan) electron microscope. Location of the individual BNNPs on the grid was carefully marked in order to analyze the same particles after high-energy Ag ion treatment.

After structural characterization, the TEM grid with BNNPs was placed in a vacuum chamber of a MEVVA-type ion implanter. The Ag ion implantation experiments were carried out at the acceleration voltages of 2, 5, 10, and 20 kV. During ion treatment, the Ar pressure was maintained at 2×10^{-2} Pa and the medium ion current was kept constant at 5 mA. In the present experiments, a not separated ion flux was used which had contained Ag ions with different charges: Ag^+ (13%), Ag^{2+} (61%), Ag^{3+} (25%), and Ag^{4+} (1%) [33]. The Ag ion flux was ~10^{14} ions/cm² × s, therefore the BNNPs received a total irradiation dose of 3×10^{16} ions/cm² over 5 min (at 5 kV). Implantation-induced structural changes within BNNPs were then thoroughly studied by TEM.

After Ag ion implantation, the samples were thoroughly characterized using a JEM ARM-200F cold field emission gun (FEG) probe and lens aberration corrected microscope operated at 200 kV. The chemical composition and distribution of Ag NPs in the BNNPs were analyzed by combination of high angle annular dark field scanning TEM (HAADF-STEM) and energy-dispersive X-ray (EDX) spectroscopy using a wide angle CENTURIO EDX detector.

2.2. Computational details

The implantation process of BNNPs by Ag ions was described in the framework of the classical molecular dynamics (MD) method with periodic boundary conditions implemented in LAMMPS [34] package. The MD simulations were carried out at a constant temperature using the Nosé-Hoover thermostat [35,36]. Temperature was chosen as 300 K to match the experimental conditions. The total time of simulation was 5 ps with the time step of 10^{-3} fs. Atomic structure was recorded every 0.5 fs. The unit cell size was ~9×4 nm² (36 *h*-BN unit cells in zigzag direction on 9 *h*-BN unit cells in armchair direction), so that the total number of atoms in the considered model was ~250,000 (~150 atomic layers of *h*-BN). The atomic interactions between B and N atoms in BNNP were described by the Tersoff 3-body potential [37] implemented in LAMMPS [38]. To describe the high energy collision between the Ag high energy ions, the smoothly splined Tersoff [39] and Ziegler-Biersack-Littmark (ZBL) [40] potentials were used. To dissipate the heat emanating from the ion cascade away from simulation, cell temperature scaling was carried out at the boundary conditions. Ag ions were placed beyond the interaction area and then were directed toward the surface with the velocity corresponding to the initial ion energy. During collisions the velocities of atoms at the boundaries were scaled to allow for the energy dissipation. Such technique allows removing the spurious pressure waves reflected from the borders of the periodic simulation cell. To avoid the displacement of the cell the atoms at borders were kept fixed [41].

Calculations of the migration barrier were performed using density functional theory within the PBE-PAW [42] approximation including the periodic boundary conditions, as implemented in the Vienna ab-initio Simulation Package [43,44]. The plane-wave energy cutoff was set to 400 eV. To calculate the equilibrium atomic structures, the Brillouin zone was sampled according to the Monkhorst-Pack [45] scheme with a k-points grid $2 \times 4 \times 2$. The structural relaxation was performed until the forces acting on each atom were less than 0.001 eV/Å. To avoid the interaction between Ag ions, the considered model consisted of three layers of *h*-BN (45 B and 45 N atoms) and Ag ion between the layers. During the calculation Ag ion was moved along the zigzag direction.

3. Results and discussion

3.1. Experimental results

HRTEM image of as-synthesized BNNPs analyzed in the present study is presented in Fig. 1. The BNNPs with an average size of 150–200 nm revealed nearly spherical morphologies with a hollow central part, and the shells (with a thickness of ~50 nm) exhibiting numerous outmost surface petals made of several stacked BN atomic layers separated by ~0.33 nm. The BNNP inner shells consisted of small highly disordered regions, several nm thick. This type of structure can be described as a turbostratic BN, with hexagonal sheets (basal planes) roughly parallel to each other but randomly rotated about the layer normal [46].

Low-magnification images of BNNPs before and after Ag ion implantation are shown in Fig. 2. It can be seen that ion irradiation did not affect the location of BNNPs; therefore the structure of the same